^{96}Zr(^{14}N,3nγ) 1979Po13

History

Type	Author	Citation	Literature Cutoff Date
Full Evaluation	Jean Blachot	NDS 109, 1383 (2008)	1-Mar-2008

E(^{14}N)=49 MeV.

^{107}Ag Levels

E(level)‡	J$^{\pi}$†	T$_{1/2}$	E(level)‡	J$^{\pi}$†	E(level)‡	J$^{\pi}$†
0.0#	1/2$^-$		1845.8 *13*		3056.1& *13*	(23/2)$^-$
93.0 *10*	7/2$^+$	44.3 s *2*	1975.5 *13*		3148.4@ *13*	(21/2)$^+$
125.4@ *13*	(9/2)$^+$		2053.4@ *13*	(17/2)$^+$	3297.8 *13*	
423.27# *6*	5/2$^-$		2297.8& *13*	(15/2)$^-$	3460.6 *13*	(23/2)$^+$
773.2@ *13*	(11/2)$^+$		2411.7& *13*	(17/2)$^-$	3466.5& *13*	(25/2)$^-$
990.9@ *13*	(13/2)$^+$		2543.0& *13*	(19/2)$^-$	3683.1 *13*	(25/2)$^+$
1146.27# *21*	(7/2,9/2)$^-$		2733.6 *13*		3928.1 *13*	
1448.8 *13*			2747.9& *13*	(21/2)$^-$	3977.9 *13*	(27/2$^+$)
1577.2 *13*	(15/2)$^+$		3028.4 *13*		4375.2 *13*	(29/2$^+$)
1799.6@ *13*	(15/2)$^+$		3034.2 *13*	$^-$	4773?	

† From γ's mult and band consideration.
‡ Level energy from least-squares adjustment.
# Band(A): p$_{1/2}$ hole band; E(levels), δ, branching ratios, HF, T$_{1/2}$ are compared with rotational-model Coriolis calc and with ^{105}Ag.
@ Band(B): g9/2 ΔJ=1 band; E(levels), δ, branching ratios, HF, T$_{1/2}$ are compared with rotational-model Coriolis calc and with ^{105}Ag.
& Band(C): 15/2$^-$ band; ΔJ=1 sequence identified up to 25/2$^-$.

γ(^{107}Ag)

A$_2$,A$_4$ coef deduced from $\gamma(\theta)$ spectra measured at nine angles between θ=+90° and −30° relative to beam axis. Transitions connect highly aligned states induced by (HI,xn)I reactions. Deorientation coef associated with A$_2$,A$_4$ coef are estimated; see 1979Po13.

E$_\gamma$	I$_\gamma$†	E$_i$(level)	J$^\pi_i$	E$_f$	J$^\pi_f$	Mult.‡	δ#	α@	Comments
(32.46)		125.4	(9/2)$^+$	93.0	7/2$^+$	M1+E2	0.074 *14*		Mult.: from adopted gammas. 1976Sv04 (^{107}Cd decay) measured γ-ray properties.
(93.1)		93.0	7/2$^+$	0.0	1/2$^-$	E3			Mult.: from adopted gammas.
113.97 *7*	27.8 *8*	2411.7	(17/2)$^-$	2297.8	(15/2)$^-$	(D+Q)	+0.05 *2*	0.2942 *14*	
120& *1*	1.2 *3*	3148.4	(21/2)$^+$	3028.4					
131.20 *5*	28.0 *3*	2543.0	(19/2)$^-$	2411.7	(17/2)$^-$	(D+Q)	+0.08 *2*	0.200 *1*	
162.8 *7*	0.9 *2*	3460.6	(23/2)$^+$	3297.8					
190.6 *2*	4.1 *4*	2733.6		2543.0	(19/2)$^-$	(D+Q)	+0.08 *7*	0.072 *1*	
205.01 *6*	23.7 *5*	2747.9	(21/2)$^-$	2543.0	(19/2)$^-$	(D+Q)	+0.09 *2*	0.0595 *2*	
217.7 *2*	14.8 *3*	990.9	(13/2)$^+$	773.2	(11/2)$^+$	(D+Q)	+0.10 *5*	0.0508 *5*	
222.5 *1*	14.6 *7*	3683.1	(25/2)$^+$	3460.6	(23/2)$^+$	(D+Q)	+0.12 *4*	0.0481 *4*	
254.1& *5*	2 *1*	2053.4	(17/2)$^+$	1799.6	(15/2)$^+$				
280.5 *5*	1.8 *3*	3028.4		2747.9	(21/2)$^-$				
294.8 *1*	12 *1*	3977.9	(27/2$^+$)	3683.1	(25/2)$^+$	(D+Q)	+0.06 *4*		

Continued on next page (footnotes at end of table)

^{96}Zr(^{14}N,3nγ) 1979Po13 (continued)

γ(^{107}Ag) (continued)

E_γ	I_γ[†]	E_i(level)	J^π_i	E_f	J^π_f	Mult.[‡]	δ[#]	α[@]	Comments
300.7 *2*	2.9 *7*	3034.2	–	2733.6		(D+Q)	+0.12 *7*		
308.15 *8*	17.8 *2*	3056.1	(23/2)$^-$	2747.9	(21/2)$^-$	(D+Q)	+0.12 *2*	0.0205 *1*	
312.21 *7*	16 *1*	3460.6	(23/2)$^+$	3148.4	(21/2)$^+$	(D+Q)	+0.17 *4*		
336.2 *4*	2.2 *8*	2747.9	(21/2)$^-$	2411.7	(17/2)$^-$				
397.0 *3*	5.4 *9*	1845.8		1448.8					
397.3 *2*	4 *2*	4375.2	(29/2$^+$)	3977.9	(27/2$^+$)	(D+Q)	+0.08 *9*		
398[&] *1*	2.9 *7*	4773?		4375.2	(29/2$^+$)				
410.3 *2*	10.7 *3*	3466.5	(25/2)$^-$	3056.1	(23/2)$^-$	(D+Q)	+0.13 *3*		
423.27 *6*	8.7 *2*	423.27	5/2$^-$	0.0	1/2$^-$	E2			Mult.: from adopted gammas.
461.6 *2*	5.4 *3*	3928.1		3466.5	(25/2)$^-$				
485.5 *2*	6.5 *2*	3028.4		2543.0	(19/2)$^-$	D+Q	+0.05 *5*		
514[&] *1*	0.9 *4*	3056.1	(23/2)$^-$	2543.0	(19/2)$^-$				
526.7 *1*	4 *1*	1975.5		1448.8		D+Q	+0.25 *5*		
586.6 *5*	6.3 *3*	1577.2	(15/2)$^+$	990.9	(13/2)$^+$	D+Q	−3.0 *9*		
612.3 *5*	4.2 *7*	2411.7	(17/2)$^-$	1799.6	(15/2)$^+$				
647.71 *5*	47.9 *5*	773.2	(11/2)$^+$	125.4	(9/2)$^+$	D+Q	+0.33 *8*		
675.7 *2*	9 *2*	1448.8		773.2	(11/2)$^+$				
(680.3)	3.2 *CA*	773.2	(11/2)$^+$	93.0	7/2$^+$				I_γ: from branching ratio: Iγ(680γ)/Iγ(648γ)=0.066 *28* (1979Sc30) via (^{6}Li,3nγ).
718.5[&] *5*	2.3 *6*	3466.5	(25/2)$^-$	2747.9	(21/2)$^-$				
723.0 *2*	9 *1*	1146.27	(7/2,9/2)$^-$	423.27	5/2$^-$	Q			
804.0 *2*	14.6 *3*	1577.2	(15/2)$^+$	773.2	(11/2)$^+$	Q			
808.5 *2*	18 *2*	1799.6	(15/2)$^+$	990.9	(13/2)$^+$	D+Q	+0.27 *8*		
865.42 *5*	100	990.9	(13/2)$^+$	125.4	(9/2)$^+$	Q			
872.1 *5*	3.3 *7*	3928.1		3056.1	(23/2)$^-$				
1026.3 *2*	3 *1*	1799.6	(15/2)$^+$	773.2	(11/2)$^+$	Q			
1062.6 *1*	34.1 *4*	2053.4	(17/2)$^+$	990.9	(13/2)$^+$	Q			
1094.9 *1*	19.4 *5*	3148.4	(21/2)$^+$	2053.4	(17/2)$^+$	Q			
1244.3 *2*	4 *1*	3297.8		2053.4	(17/2)$^+$				
1306.9 *1*	42.5 *4*	2297.8	(15/2)$^-$	990.9	(13/2)$^+$	D+Q	−0.01 *2*		

[†] From γ singles and $\gamma\gamma$ coin spectra at 49 MeV; doublets and contaminants are resolved via $\gamma\gamma$ coin, cross bombardments, and excit.

[‡] Determined from $\gamma(\theta)$ and $\gamma\gamma(\theta)$ ratio data, except as noted. Quadrupole transitions, interpreted as E2, are characterized by A_2=+0.2 to +0.35. A highly mixed transition is assigned as M1+E2 since E1+M2 is unlikely.

[#] Deduced from $\gamma(\theta)$ or $\gamma\gamma(\theta)$ ratio if composite γ ray;

[@] Total theoretical internal conversion coefficients, calculated using the BrIcc code (2008Ki07) with Frozen orbital approximation based on γ-ray energies, assigned multipolarities, and mixing ratios, unless otherwise specified.

[&] Placement of transition in the level scheme is uncertain.

^{96}Zr(^{14}N,3nγ) 1979Po13

Level Scheme

Intensities: Type not specified

Legend

$I_\gamma < 2\% \times I_\gamma^{max}$

$I_\gamma < 10\% \times I_\gamma^{max}$

$I_\gamma > 10\% \times I_\gamma^{max}$

γ Decay (Uncertain)

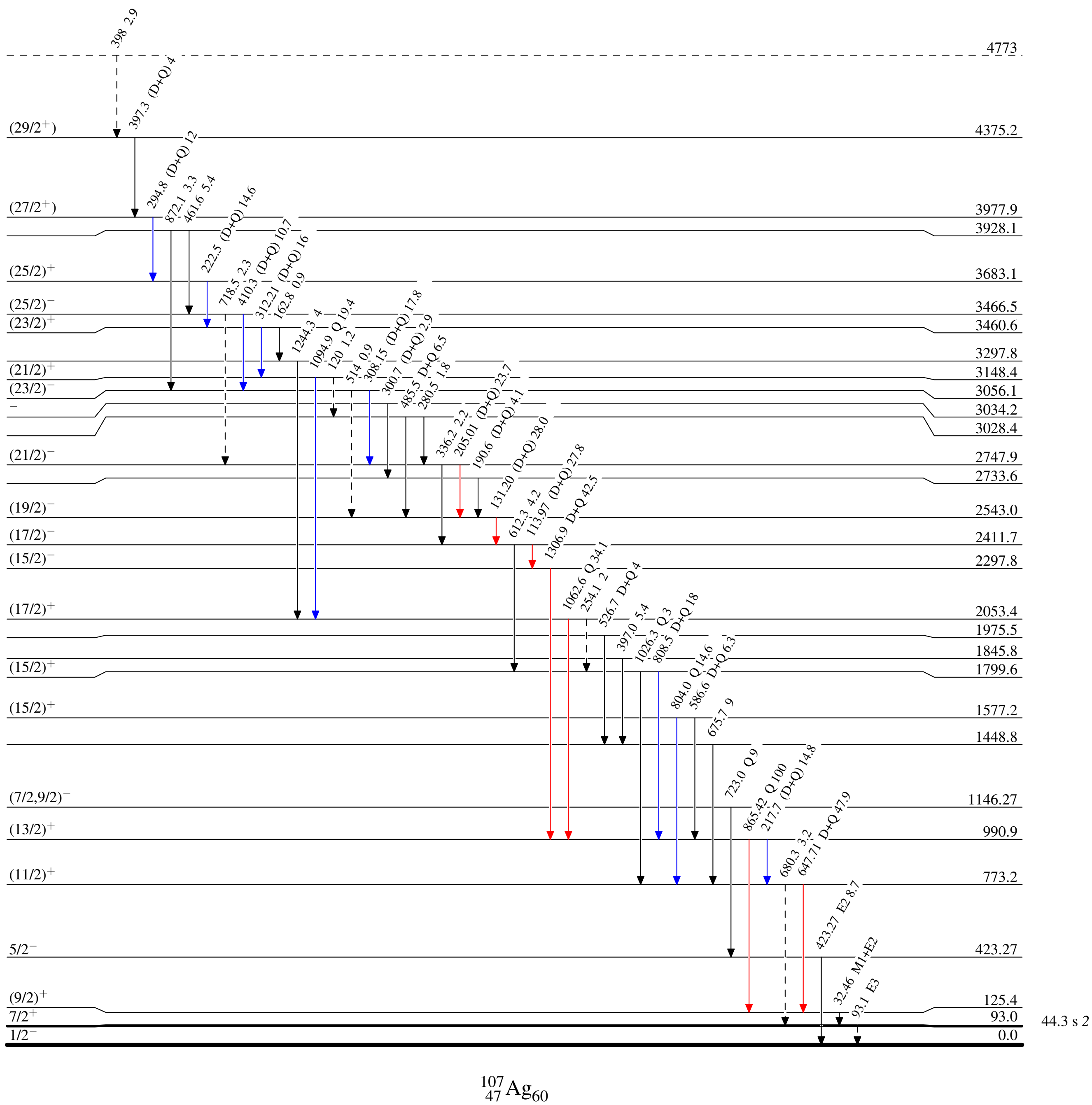

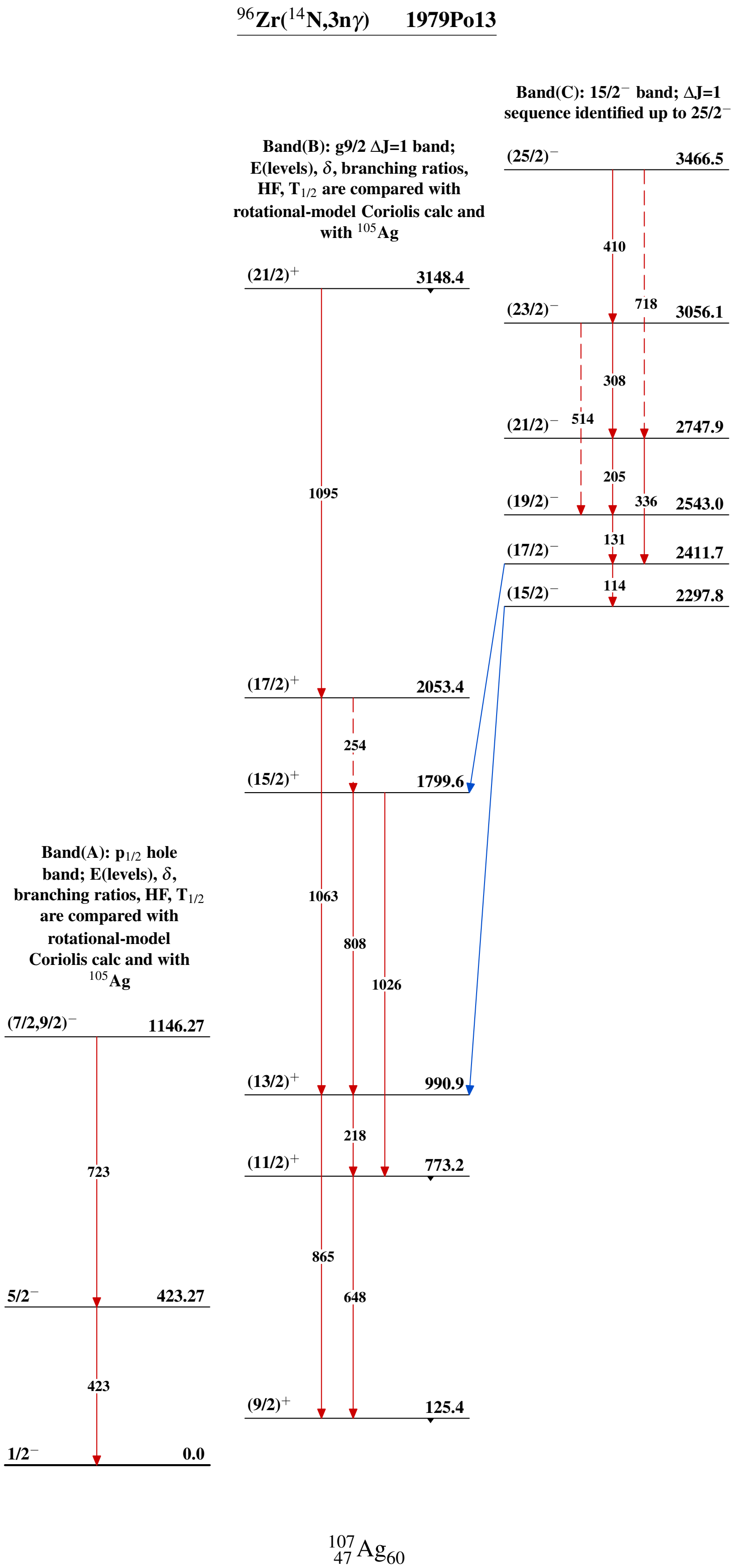
^{96}Zr(^{14}N,3nγ) 1979Po13
Band(C): 15/2⁻ band; ΔJ=1 sequence identified up to 25/2⁻
Band(B): g9/2 ΔJ=1 band; E(levels), δ, branching ratios, HF, $T_{1/2}$ are compared with rotational-model Coriolis calc and with ^{105}Ag
Band(A): $p_{1/2}$ hole band; E(levels), δ, branching ratios, HF, $T_{1/2}$ are compared with rotational-model Coriolis calc and with ^{105}Ag
(25/2)⁻ 3466.5
(23/2)⁻ 3056.1
(21/2)⁻ 2747.9
(19/2)⁻ 2543.0
(17/2)⁻ 2411.7
(15/2)⁻ 2297.8
(21/2)⁺ 3148.4
(17/2)⁺ 2053.4
(15/2)⁺ 1799.6
(13/2)⁺ 990.9
(11/2)⁺ 773.2
(9/2)⁺ 125.4
(7/2,9/2)⁻ 1146.27
5/2⁻ 423.27
1/2⁻ 0.0
410
718
308
514
205
336
131
114
1095
254
1063
808
1026
218
865
648
723
423
$^{107}_{47}Ag_{60}$